

# Design of Artificial Apposition Compound Eye with Cylindrical Micro-Doublets

Anel GARZA-RIVERA\* and Francisco-J RENERO-CARRILLO

*Instituto Nacional de Astrofísica, Óptica y Electrónica, Luis Enrique Erro #1,  
Santa María Tonantzintla, 72840 Puebla, México*

(Received May 31, 2010; Revised July 19, 2010; Accepted July 24, 2010)

We present the design of a non-conventional optical system that uses cylindrical micro-doublets (CMD), integrated in an artificial apposition compound eye configuration (AACE). We show some designs of an ultra-thin objective inspired in fly eyes. These designs can give options to create new technologies that will process information in a different and effective way as usual. This process will be carried out by means of sampling the object with an array of multiple micro lenses using a certain value of the acceptance angle, and processing the optical signal to obtain partial images that will be part of a global one. The objective has the advantage of having a smaller size, a wider field of view, and an acceptable image quality compared with some conventional systems. Design parameters of the AACE and optical performance of the CMD are reported. © 2011 The Japan Society of Applied Physics

**Keywords:** apposition compound eye, camera micro-objective, optical design

## 1. Introduction

Technological advances in manufacturing and material science have allowed the development of micro-optical systems. Many of them are already incorporated in common use devices such as micro cameras, spy cameras, micro-scanners.<sup>1–4)</sup> In this miniaturizing trend, non-conventional optical systems offer an alternative to built very compact size imaging systems with a reliable quality that could be used in many applications like Chip cards, clocks, automobile industry, etc.<sup>5)</sup> Herein, we present the designs of an ultra-thin planar apposition compound eye as an objective based in the concept of cylindrical micro-doublets (CMD). The CMD can be considered as the optical unit of apposition compound eyes.<sup>3,4)</sup> We based our work in the anatomy and function of the natural apposition compound eye that some insects have, and in previous papers from Duparré and coworkers<sup>3–5)</sup> and Tanida and coworkers.<sup>6,7)</sup>

We present here the basic concepts of the apposition compound eye, we evaluate the optical performances of the CMD for three different refractive indexes for the first lens element, and finally we show the parameters for the optical design of the objectives. For the design process, we calculated the dimensions of the elements of the CMD, like aperture diameter  $D$ , Radius of curvature  $R$ , and refractive indexes  $n_1$  and  $n_2$ . We evaluated the optical performance of the element and we observed the aberrations and the spot diagram produced by the CMD.

We introduced opaque walls between channels, and we considered their thickness to be able to calculate the final number of units  $N$  that would integrate the objective. We had to take in consideration the detector size. We used a small piece of detector that consisted of 500 pixels, each of  $5\mu\text{m}$ . and for a second case we used 5000 pixels. We continued calculating the pinhole diameter  $d_{\text{Airy}}$ , the accept-

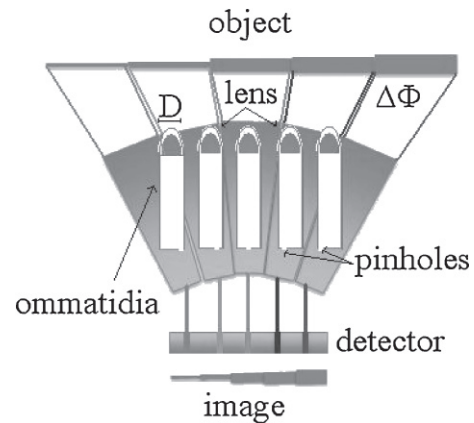


Fig. 1. Diagram of sampling of the object and image formation by the natural apposition compound eye where:  $\Delta\Phi$  interommatidial angle, and  $D$  diameter of the microlens. We show the planar array with micro doublets and pinholes that will form the AACE.

ance angle  $\Delta\phi$ , the FOV, the pinhole pitch  $P_P$ , the pitch difference  $\Delta P$ , the interommatidial angle  $\Delta\Phi$ , the sampling frequency  $\nu_s$ , and the pinhole position  $X_N$ . The parameters that give more information about the optical performance of the system are  $\Delta\phi$ ,  $\Delta\Phi$ , and  $\nu_s$ .

## 2. Apposition Compound Eye Visual Unit

Apposition eyes consist of an array of lenses and photoreceptors. The combination of one lens and one photoreceptor forms a unit called ommatidium. Figure 1 shows pattern diagrams for illustrative purposes of how a natural apposition compound eye works. Each small lens focuses light from a small solid angle  $\Delta\phi$  of object space onto a single photoreceptor. The angular object space is sampled with the interommatidial angle  $\Delta\Phi$ . The field of view (FOV) of this imaging system is determined by the radius of curvature  $R$  and size of the eye.<sup>4)</sup>

\*E-mail address: anelgarza@inaoep.mx

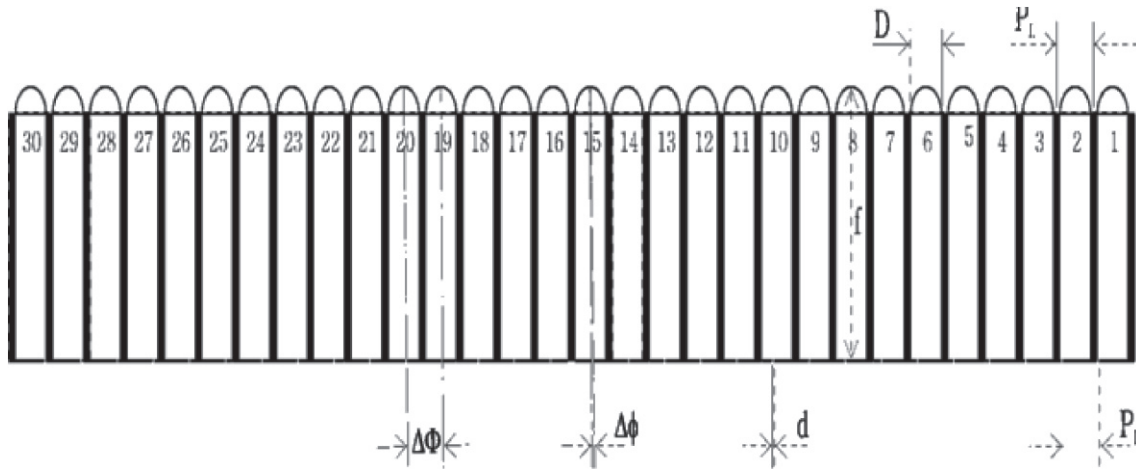


Fig. 2. Planar artificial apposition compound eye objective, where:  $\Delta\Phi$  interommatidial angle,  $\Delta\phi$  acceptance angle,  $D$  diameter of the microlens,  $f$  focal length,  $d$  pinhole diameter,  $P_p$  pinhole pitch and  $P_L$  microlens pitch.

### 3. Artificial Apposition Compound Eye with Microlens and Pinholes Arrays with a Planar Configuration

We have designed three artificial apposition compound eyes (AACE), composed by many CMD units, with a thickness of the system that will not be more than  $350\ \mu\text{m}$ . The objective consists of a polymer microlens array over a glass substrate (opaque walls between the channels are required), and on the edge, a metallic plate with a pinhole array.<sup>4)</sup> The image is recorded by a photodetector just after the pinhole array. The most important use of the AACE is to form an ultrathin objective with very low volume, high sensitivity and that gives images with acceptable resolution.

#### 3.1 Description of the system and designing issues

To design the AACE we considered,<sup>3-5)</sup> the angular resolution ( $\Delta\Phi$ ), which is defined by the interommatidial angle;

$$\Delta\Phi = \arctan\left(\frac{\Delta P}{f}\right), \quad (1)$$

where  $\Delta P$  is the pitch difference, and  $f$  is the microlens focal length (see Fig. 2). The acceptance angle ( $\Delta\phi$ ) of one ommatidia is given by

$$\Delta\phi = \left[ \left(\frac{d}{f}\right)^2 + \left(\frac{\lambda}{D}\right)^2 \right]^{1/2}, \quad (2)$$

where  $\lambda$  is the wavelength of light coming from the source,  $d$  is the pinhole diameter, and  $D$  is the microlens diameter. The pinhole diameter is calculated by means of Airy disk

$$d_{\text{Airy}} = 2.44 \frac{\lambda f}{D}, \quad (3)$$

the pitch difference is given by

$$\Delta P = P_L - P_p, \quad (4)$$

the pinhole array for an objective with  $N$  channels in one dimension is calculated with

$$P_p = a \left\{ 1 - \left[ \frac{N}{(N+1)} \right] \right\}, \quad (5)$$

where  $a$  is the detector length. We based our calculations in a detector unit of 500 pixels with a pixel size of  $5\ \mu\text{m}$ . The position of the pinholes can be calculated according to the position of the lens.<sup>8)</sup>

a) Measuring from the left side:

$$X_N = N_L \Delta P, \quad (6)$$

where  $X_N$  is the position of the  $N$  pinhole measured from the left side,  $N_L$  is the corresponding CMD unit and  $\Delta P$  is the pitch difference.

a) Measuring from the right side:

$$Y_N = N_L P_p, \quad (7)$$

where  $Y_N$  is the position of the  $N$  pinhole measured from the right side,  $N_L$  is the corresponding CMD unit and  $P_p$  is the pinhole pitch.

### 4. Improving the Cylindrical Micro-Doublets

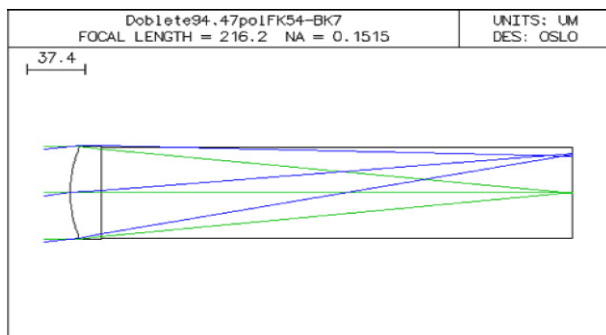
We designed three different CMD<sup>8)</sup> to minimize the aberrations and the size of the spot diagram produced by the objective. We use different materials for the first lens element, while the refractive index of the substrate does not change. The ray tracing was done by using OSLO Premium Edition 6.2. The Slider Wheel Menu was used to optimize the spot size. In Fig. 3(a) we illustrate how light is focused in the CMD, and in Fig. 3(b) we show that the spot size in the optical axis will give a good image quality.

### 5. Results

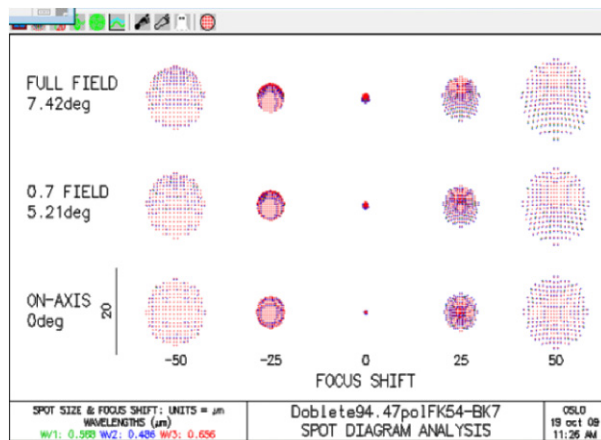
The parameters of our designs were calculated using the equations above. The position of the pinholes depends on the area that is not covered by the opaque walls used to avoid crosstalk, and we have to consider their thickness. Table 1 shows the design parameters of the three objectives, we see that the performance of the AACE can be estimated by the

Table 1. Parameters of artificial apposition compound eye objectives.<sup>8)</sup>

Design parameters	AACE1	AACE2	AACE3
f-number $F\#$	3.3	3.3	3.3
Number of channels $N$ (for a detector with 5000 pixels)	$25 \times 25$	$30 \times 30$	$30 \times 30$
Aperture diameter $D$ ( $\mu\text{m}$ )	70	65.5	68.5
Radius of curvature $R$ ( $\mu\text{m}$ )	102.4	94.5	119.4
Thickness $f$ ( $\mu\text{m}$ ) (corresponds to focal length)	340	320	320
Microlens pitch $P_L$ ( $\mu\text{m}$ )	100	84	84
Pinhole diameter $d$ ( $\mu\text{m}$ )	2.8	2.7	2.7
Refractive Index spacing structure microlens, pinhole ( $n_2$ )	1.5168	1.5168	1.5168
Refractive Index replicated microlens ( $n_1$ )	1.4370	1.4370	1.5638
Field of view FOV (deg)	19	14.71	14.71
Thickness of opaque walls for prevention of crosstalk $w_{th}$ ( $\mu\text{m}$ )	30	18.5	15.5
Interommatidial angle $\Delta\Phi$ (deg)	0.4718	0.4834	0.4834
Acceptance angle $\Delta\phi$ (deg)	0.673	0.937	0.937
Sampling frequency $\nu_s$ (cycle/rad)	44.27	59.26	59.26



(a)



(b)

Fig. 3. (Color online) (a) Configuration of the CMD used for the AACE2. (b) Spot size produced by the AACE2 in focus that fits the Airy disk.

interommatidial and acceptance angle values, using the Nyquist criterion, and the quality of the image depends on the sampling frequency.

## 6. Conclusions

To obtain a better optical performance of the AACE objective designs, we optimized the CMD with OSLO to minimize the aberrations. We combined different values of the refractive index using different materials (acrylate polymers), and we tried to keep the objectives as thin as possible. The objectives have a wider FOV compared with a conventional unique aperture camera. The sampling frequency is between 44 and 60 cycle/rad, which is an acceptable value according to Nyquist criterion. We expect a better performance, and lower values of the aberrations using aspherization in the CMD designs, which can make fabrication more difficult. The AACE could be fabricated using lithographical processes on a wafer scale.<sup>3,4)</sup> The thickness of the wafer corresponds to the focal length in the polymer. The microlens arrays generation involves many steps, including master and mold generation and subsequent replication. Fabrication presents limitations to viable geometries.

## References

- 1) G. Molar, F. Renero, and W. Calleja: *Optik* **2** (2010) 843.
- 2) J. Tanida, T. Kumagai, K. Yamada, and S. Miyatake: *Appl. Opt.* **40** (2001) 1806.
- 3) J. Duparré, P. Dannberg, P. Schreiber, A. Bräuer, and A. Tünnermann: *Appl. Opt.* **43** (2004) 4303.
- 4) J. Duparré, P. Dannberg, P. Schreiber, A. Bräuer, and A. Tünnermann: *Appl. Opt.* **44** (2005) 2949.
- 5) J. Duparré and R. Völkel: *Novel Optics/Micro-Optics for Miniature Imaging Systems* [www.suss\_microoptics.com].
- 6) R. Horisaki, Y. Nakao, T. Toyoda, and J. Tanida: *Opt. Rev.* **16** (2009) 241.
- 7) Y. Kitamura, R. Shogenji, K. Yamada, and J. Tanida: *Appl. Opt.* **43** (2004) 1719.
- 8) A. Garza-Rivera: Master Dissertation, Instituto Nacional de Astrofísica, Óptica y Electrónica, Puebla, Mexico (2009) [in Spanish].